CrossMark

ORIGINAL RESEARCH

Magnetic and magnetocaloric properties of nano-sized $La_{0.8}Ca_{0.2}Mn_{1-x}Fe_xO_3$ manganites prepared by sol–gel method

D. Fatnassi[1,3] · Kheiria Sbissi[1] · E. K. Hlil[2] · M. Ellouze[1] ·
J. L. Rehspringer[3] · F. Elhalouani[4]

Abstract We present an investigation on magnetic and magnetocaloric properties of nano-sized $La_{0.8}Ca_{0.2}Mn_{1-x}Fe_xO_3$ ($x = 0$, 0.01, 0.15, 0.2) manganites synthesized by sol–gel process. X-ray diffraction and magnetization measurements were performed to investigate both crystallographic structure and magnetocaloric properties, respectively. All samples show an orthorhombic structure with Pnma space group. Ferromagnetic–paramagnetic transition sensitive to iron doping is observed at Curie temperature (T_C) ranging from 223 K ($x = 0$) to 70 K ($x = 0.2$). In addition, a large magnetocaloric effect near T_C is observed. Under a magnetic field change of 5 T, a maximum of magnetic entropy ΔS_M^{max} reaches 4.42, 4.32, 1.6, and 0.54 J kg^{-1} K^{-1}, for $x = 0$, $x = 0.01$, $x = 0.15$, and $x = 0.2$, respectively. The relative cooling power (RCP) values were computed as well. RCP values of 164 and 117 J kg^{-1} were found for $La_{0.8}Ca_{0.2}MnO_3$ (LCM) and $La_{0.8}Ca_{0.2}Mn_{.99}Fe_{0.01}O_3$ (LCMFe$_{0.01}$), respectively. The large values of entropy changes and related RCP allow concluding that our material could be a highly attractive candidate for magnetic refrigeration.

✉ D. Fatnassi
  fatnassidad@yahoo.fr

1 Faculty of Sciences of Sfax, Sfax University,
  BP 1171-3000, Sfax, Tunisia

2 Institute Néel, CNRS et Université Joseph Fourier, BP 166,
  38042 Grenoble Cedex 9, France

3 Institute of Physics and Chemistry of Materials of Strasbourg,
  UMR 7504 CNRS Université de Strasbourg, BP 43,
  67034 Strasbourg Cedex 2, France

4 National Engineering School of Sfax, BP W, 3038 Sfax,
  Tunisia

Introduction

The modern society is increasingly relying on refrigeration technology. The vapor compression refrigerators have been mainly used for cooling applications. However, the compression and expanding processes in the refrigerators of a gas are not sufficiently efficient. On the other hand, the use of gases such as chlorofluorocarbons and hydro-chlorofluorocarbons is damaging to our living environment. For these reasons, exploring a new type refrigeration technology that is environmentally friendly and energy efficient becomes an urgent necessity. Comparing to the conventional gas compression (CGC), magnetic refrigeration (MR) based on the magnetocaloric effect (MCE) [1] exhibits several advantages [2, 3]. Indeed, the MR does not use global warming gases and therefore is an environmentally friendly cooling technology [4, 5]. So an ongoing research is necessary to find appropriate materials with a large enough magnetic entropy at moderate magnetic fields near room temperature [5, 6]. The gadolinium (Gd) rare earth metal has been considered as the most obvious material exhibiting a large MCE in room-temperature magnetic refrigerators [2, 7, 8]. However, the use of the Gd is limited due to its expensive cost price. Nevertheless, some other candidates have been found to exhibit large MCE, such as $Gd_5(Si_xGe_{1-x})_4$ [9], $La(Fe_{1-x}Si_x)_{13}$ [10], $MnFeP_{1-x}As_x$ [11], and $Tb_{1-x}Gd_xAl_2$ [12].

In the last few years, manganites with a general formula $R_{1-x}A_xMnO_3$ (R = rare earth, A = alkali earth) have attracted more attention as alternative candidates for MR near room temperature. Compared to Gd, they show several advantages such as higher chemical stability, higher

🍃 Springer

resistivity, and lower cost. Their preparation can be achieved without substantial difficulties. As other advantages, they present the possibility to tune their magnetic transition temperature by the substitution on both R-sites and Mn-sites. The MCE of $La_{1-x}A_xMnO_3$ (A = Ca, Sr, Ba) manganites was first studied by Moreli et al. [13]. A large MCE in $La_{1-x}A_xMnO_3$ polycrystalline samples ($0.2 \leq x \leq 0.33$) is reported by Guo et al. [14, 15]. In fact, for $\Delta H = 1.5$ T, the $|\Delta S_M|$ reaches a maximum of about 5.5 J/(kg K) at 230 K, 4.7 J/(kg K) at 224 K, and 4.3 J/(kg K) at 260 K for $x = 0.2, 0.25$, and 0.33, respectively [14]. For the same magnetic field of 1.5 T, these values are larger than that of Gd, $|\Delta S_M| = 4.2$ J/(kg K) [2]. As other significant information, the magnitude of $|\Delta S_M|$ was found to be inversely proportional to the grain size [16]. This paper is devoted to seeking for new perovskite manganites with broad refrigerant capacity and large MCE demanding only low applied magnetic fields close to the room temperature. Precisely, we report the effect of Fe doping on the magnetic and magnetocaloric properties of $La_{0.8}Ca_{0.2}Mn_{1-x}Fe_xO_3$ ($x = 0, 0.01, 0.15, 0.2$). They present large magnetic entropy change values and high relative cooling power (RCP) factors.

Experimental

The nano-sized $La_{0.8}Ca_{0.2}Mn_{1-x}Fe_xO_3$ ($x = 0, 0.01, 0.15, 0.2$) manganites were synthesized using the sol–gel method. The starting precursor MnO_2 was mixed in appropriate proportion and dissolved in the concentrated nitric acid. Suitable amounts of citric acid and ethylene glycol, as a coordinate agent, were added. After the addition of the other precursors La_2O_3, $CaCO_3$, and Fe_2O_3, a clear black stained solution was obtained. Then the solution is allowed to dry to form a dried gel, followed by baking at 170° C to obtain black precursor powder. Finally, the resulting powder was heated in air at 950 °C for 24 h. The X-ray diffraction patterns at room temperature were obtained using SIEMENS D8 X-ray diffractometer with Cu Kα radiation. The FULLPROF program based on the Rietveld method [17] was used for phase analysis. The magnetic isotherms were recorded in the magnetic field of up to 5 T and at the temperature ranging from 4 to 400 K. The magnetocaloric effects (MCE) were estimated via the Maxwell relation [2].

Results and discussion

X-ray diffraction

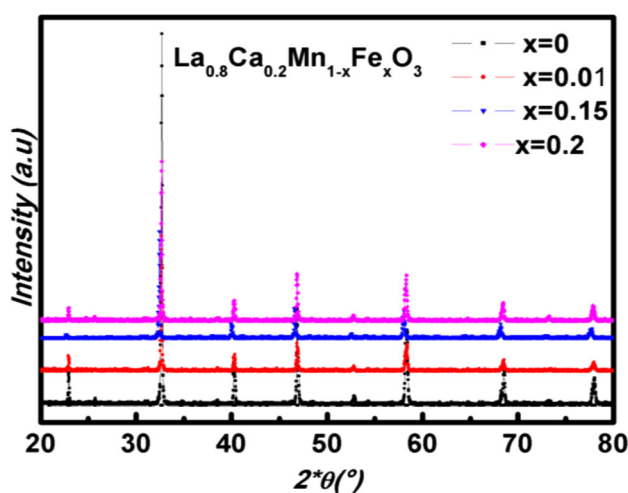Powder X-ray diffraction patterns (Fig. 1) show that the samples show single phase and indexed in the

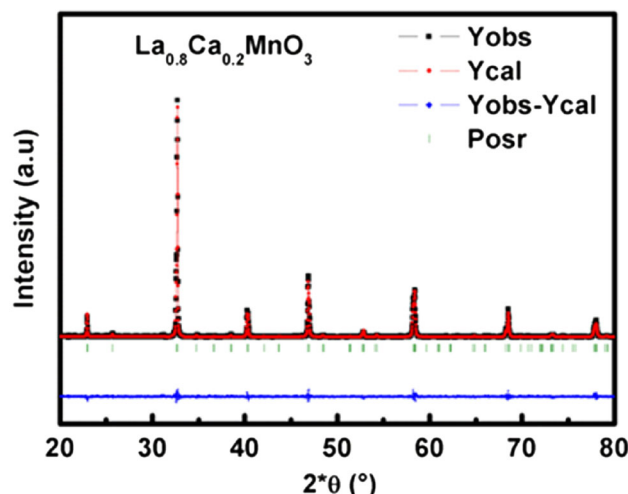**Fig. 1** Powder X-ray diffraction patterns for $La_{0.8}Ca_{0.2}Mn_{1-x}Fe_xO_3$ ($x = 0, 0.01, 0.15, 0.2$)

Fig. 2 Observed (*solid symbols*) and calculated (*solid lines*) X-ray diffraction pattern for $La_{0.8}Ca_{0.2}MnO_3$ sample. Positions for the Bragg reflections are markedly *vertical bars*. Differences between the observed and the calculated intensities are shown at the *bottom* of the figure

orthorhombic structure with Pnma group space (Fig. 2). Refined cell parameters such as unit cell parameters, unit cell volume, R factor, and the goodness-of-fit indicator (χ^2) are listed in Table 1. We can deduce that the substitution of Mn^{3+} by Fe^{3+} ions induces an increase of the unit cell volume. The linear increase is unexpected because we substitute Mn^{3+} having 0.0645 nm as ionic radius by Fe^{3+} with the same ionic radius (0.0645 nm). Consequently, no change induced by this substitution is expected. Therefore, the increase could be attributed to the lattice disorder arising from the random occupancy of Fe and Mn ions on the B-site. Indeed, in the pure perovskite $La_{0.8}Ca_{0.2}MnO_3$

Table 1 Refined structural parameters of $La_{0.8}Ca_{0.2}Mn_{1-x}Fe_xO_3$ ($x = 0$, 0.01, 0.15, 0.2) compounds

Samples	$x = 0$	$x = 0.01$	$x = 0.15$	$x = 0.2$
a (Å)	5.46936	5.46979	5.47419	5.47565
b (Å)	7.7337	7.73569	7.74508	7.74596
c (Å)	5.4935	5.49399	5.49581	5.49606
V (Å^3)	232.366	232.465	233.012	233.119
χ^2	1.47	1.4	1.14	1.12
Rf	5.73	6.32	11.5	6.8

system (LCMO), Mn shows a mixed valence with Mn^{3+}/Mn^{4+} ratio close to 4 ($[Mn^{4+}] = 0.2$ and $[Mn^{3+}] = 0.8$) with a valence of +3 for La. The partial substitution of the Mn ions by transition metal ions (Fe) in $La_{0.8}Ca_{0.2}Mn_{1-x}Fe_xO_3$ manganites gives rise to changes in the Mn^{3+}/Mn^{4+} rate, and some Mn^{3+}–O^{2-}–Mn^{4+} networks are substituted by Fe^{3+}–O^{2-}–Mn^{4+}. This causes a disorder of the charge transfer mechanism. Such disorder causes a change in the Mn–O distances and Mn–O–Mn angles. Consequently, the distortion of the ideal perovskite structure in which the Mn–O–Mn angle is equal to 180° undergoes a modification. These results are similar to those obtained by Othmani et al. [18].

Magnetic properties

To study the effect of substitution of iron in manganese sites on the magnetic properties, we have analyzed the magnetization variation versus temperature of $La_{0.8}Ca_{0.2}Mn_{1-x}Fe_xO_3$ ($x = 0$, 0.01, 0.15, 0.2) samples under an applied magnetic field of $H = 0.05$ T (Fig. 3). The M (T) curves reveal that all samples exhibit a ferromagnetic (FM)–paramagnetic (PM) transition at Curie
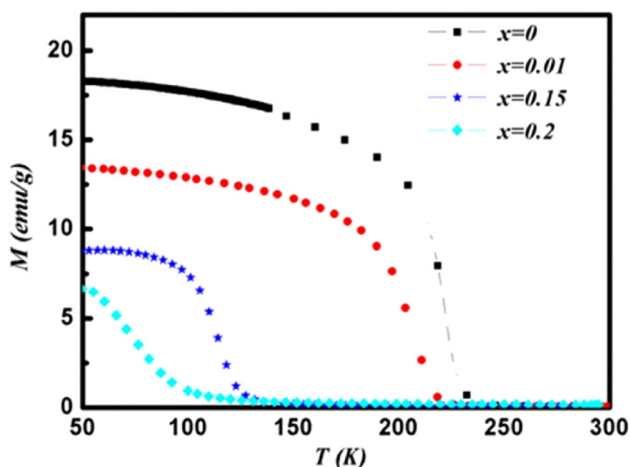
Fig. 3 Magnetization versus temperature for $La_{0.8}Ca_{0.2}Mn_{1-x}Fe_xO_3$ ($x = 0$, 0.01, 0.15, 0.2) samples under 0.05 T

temperature, $T_C = 223$, 205, 114, and 70 K, for $x = 0$, 0.01, 0.15, 0.2, respectively. The Curie temperature T_C, defined as the peak of dM/dT in the M (T) curves, is reported for all compositions in Table 3. This table gives evidence that T_C and the magnetization are sensitive to Fe content. Indeed, the increase in Fe content causes an increase in T_C accompanied by a reduction of the magnetization. Probably, both changes are attributed to the competition between the superexchange (Mn^{4+}–O–Mn^{4+}) and double-exchange (Mn^{3+}–O–Mn^{4+}) interactions. The Fe takes place at the Mn site as Fe^{3+} (replacement of some Mn^{3+}–O–Mn^{4+} bonds by Mn^{4+}–O–Fe^{3+} bonds), giving rise to an antiferromagnetic coupling between Mn and Fe ions that favors the superexchange mechanism. The evolution of magnetization (M) versus the applied magnetic field (μ_0H) for $x = 0$, 0.01, 0.15, and 0.2 samples, obtained at different temperatures and measured under applied magnetic field ranging from 1 to 5 T, is shown in Fig. 4. These curves show that, below the Curie temperature, the magnetization greatly increases with the magnetic field and the saturated M is reached at $H = 1$ T. For $T > T_C$, the variation of M (T, μ_0H) does not reach the saturation and a linear behavior appears. This result confirms that all samples present a typical ferromagnetic behavior.

Figure 5 presents the magnetization measurements performed at 4 K under applied magnetic fields of up to 6 T, for $La_{0.8}Ca_{0.2}Mn_{1-x}Fe_xO_3$ ($x = 0$, 0.01, 0.15, 0.2) samples. Table 2 lists the experimental and the calculated magnetic moments per Mn ion, denoted by M_{Sat}^{Exp} and M_{Sat}^{Theo}, respectively. The values of M_{Sat}^{Theo} have been calculated by considering that the spins of all Mn and Fe ions are aligned. The magnetic moment of $La_{0.8}^{3+}Ca_{0.2}^{2+}(Mn_{1-x}Fe_x)_{0.8}^{3+}Mn_{0.2}^{4+}O_3$ is expressed as

$$M_{Sat}^{Theo} = [4 \times (0.8 - 0.8 \times x) - 5 \times (0.8 \times x) + 3 \times (0.2)]\mu_B$$
$$= (3.8 - 7.2 \times x)\mu_B.$$

(1)

The magnetic moments of Mn^{3+}, Mn^{4+}, and Fe^{3+} ions are $\mu_{Mn}^{3+} = 4\mu_B$, $\mu_{Mn}^{4+} = 3\mu_B$, and $\mu_{Fe}^{3+} = 5\mu_B$, respectively. The x is the iron concentration and μ_B is the Bohr magneton. We note that the magnetization saturation values M_{Sat} decrease with increasing Fe content, especially for $x = 0.2$. It is worth noting that similar results are reported in [19]. The difference between the measured and the calculated values should be explained by the presence of a magnetic inhomogeneity or by spin-canted state at low temperature.

Arrott curve

To determine the nature of magnetic transition type (first or second order), we have considered the experimental
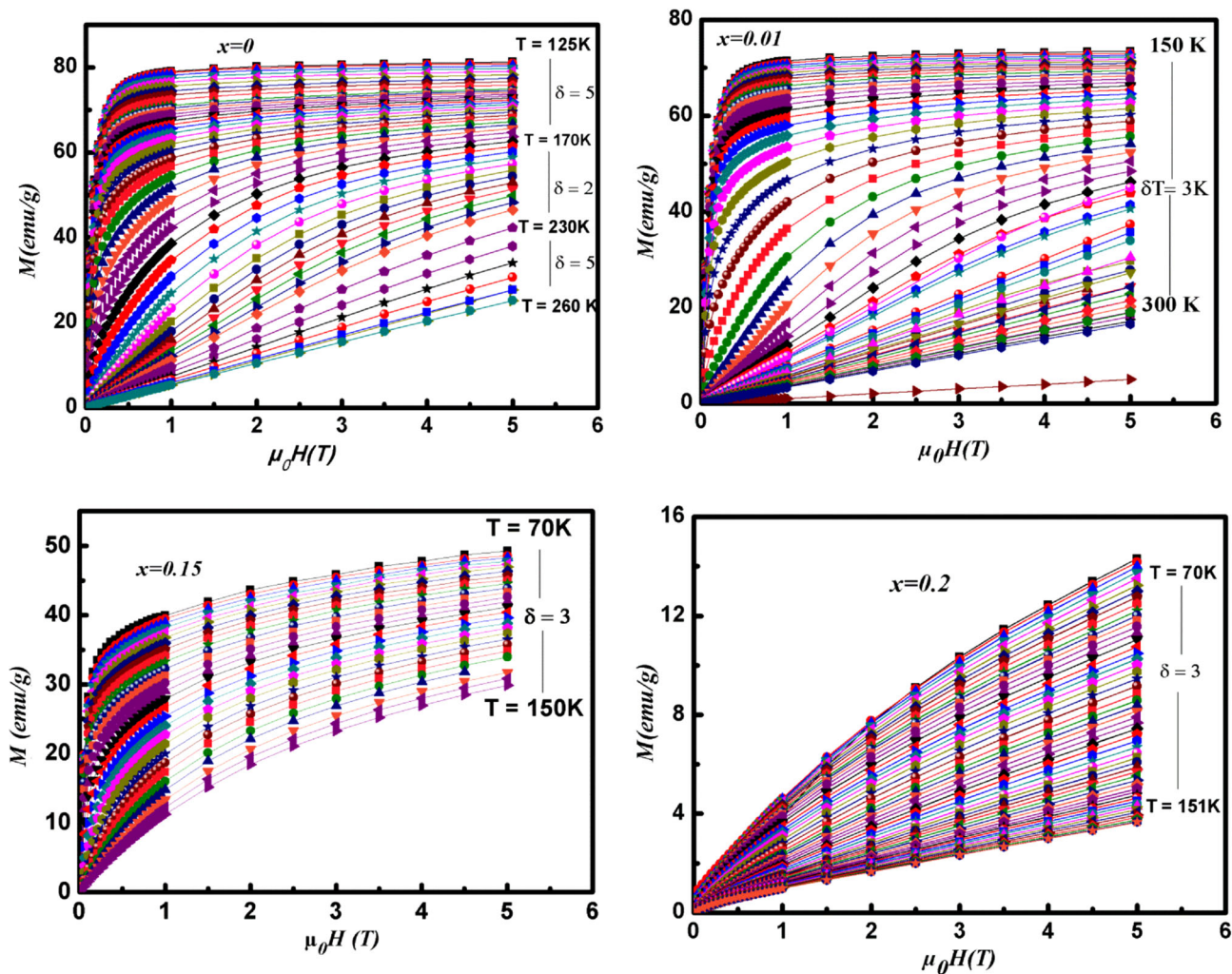
Fig. 4 Isothermal magnetization M (H) for $La_{0.8}Ca_{0.2}Mn_{1-x}Fe_xO_3$ samples at different temperatures: **a** $x = 0$, **b** $x = 0.01$, **c** $x = 0.15$, and **d** $x = 0.2$

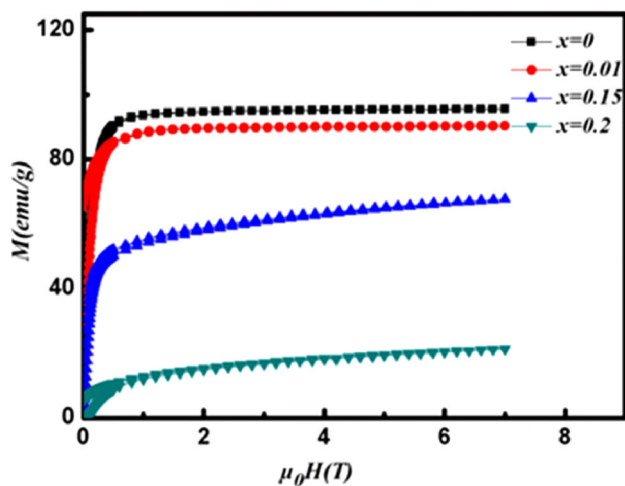**Fig. 5** Magnetization versus applied magnetic field at 4 K for $La_{0.8}Ca_{0.2}Mn_{1-x}Fe_xO_3$ ($x = 0, 0.01, 0.15, 0.2$) samples

Table 2 Experimental and theoretical saturated magnetization moment

Samples	$M_{Sat}^{Exp}(\mu_B)$	$M_{Sat}^{Theo}(\mu_B)$
$x = 0$	3.75	3.8
$x = 0.01$	3.6	3.728
$x = 0.15$	2.3	2.72
$x = 0.2$	0.36	2.36

criterion given by Banerjee [20]. It consists in inspecting the slope of isotherm plots of μ_0H/M versus M^2. According to this criterion, magnetic transition is of second order if all the curves have positive slopes, while, if some of these curves show a negative slope, the transition is first order. Figure 6 shows the isotherm M^2 versus μ_0H/M above and below T_C for $La_{0.8}Ca_{0.2}Mn_{1-x}Fe_xO_3$ ($x = 0, 0.01, 0.15$)
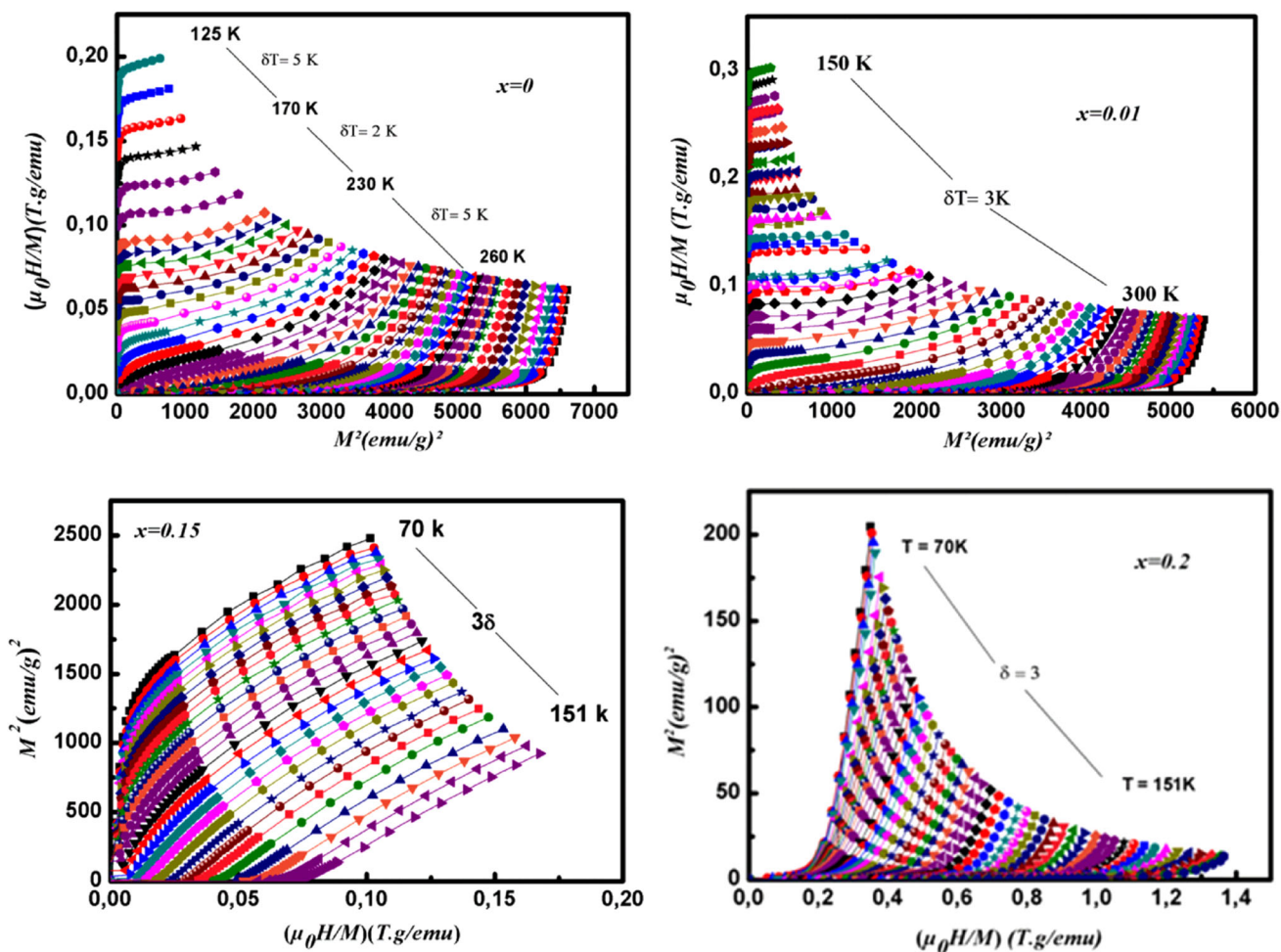
Fig. 6 Arrott curves M^2 versus $\mu_0 H/M$ for La$_{0.8}$Ca$_{0.2}$Mn$_{1-x}$Fe$_x$O$_3$ samples: **a** $x = 0$, **b** $x = 0.01$, **c** $x = 0.15$, and **d** $x = 0.2$

samples. Based on the of Banerjee's criterion, the LCM and LCMF$_{0.01}$ systems exhibit a first-order ferromagnetic-to-paramagnetic phase transition, whereas a second-order transition is confirmed for LCMF$_{0.15}$ and LCMF$_{0.2}$.

Magnetocaloric study

The MCE is defined as the heating or cooling of a magnetic material due to the application or suppression of a magnetic field, respectively. To estimate the magnetocaloric effect, the change of magnetic entropy (ΔS_M) was calculated numerically using the equation [21]:

$$-\Delta(S_M) = \sum \frac{(M_i - M_{i+1})}{T_{i+1} - T_i} \Delta H_i. \tag{2}$$

The M_i and M_{i+1} are the experimental values of magnetization measured at temperatures T_i and T_{i+1}, respectively. The H_i is the applied magnetic field. The magnetic entropy change (ΔS_M) determined numerically using Eq. (2) and the M (T, $\mu_0 H$) curves are shown in Fig. 7. The

(ΔS_M) value increases with temperature increase to reach a maximum near T_C and lowers above T_c. To compare our results with previously published data for other perovskite manganites, we listed in Table 3 the data of several magnetic materials that could be used as magnetic refrigerants. Also, the maximum magnetic entropy change of Fe-doped manganites increases gradually with increasing applied magnetic field for such materials. We noted that the maximum entropy change $\left| \Delta S_M^{max} \right|$ corresponding to a magnetic field variation of 5 T for La$_{0.8}$Ca$_{0.2}$MnO$_3$ and La$_{0.8}$Ca$_{0.2}$Mn$_{0.99}$Fe$_{0.01}$O$_3$ is about 4.42 and 4.32 J/(kg K), respectively.

In Table 3, we compared our performances of MCE with those of Gd [2]-based materials as well as rare earth manganites. The highest value of the magnetic entropy change for La$_{0.8}$Ca$_{0.2}$MnO$_3$ and La$_{0.8}$Ca$_{0.2}$Mn$_{0.99}$Fe$_{0.01}$O$_3$ samples is observed with $x = 0$ content and is equal to 1.96 and 4.42 J/(kg K) under magnetic fields of 1 and 5 T, respectively. In addition, similar results were observed by Shaobo Xi et al. for La$_{0.8}$Ca$_{0.2}$MnO$_3$ [25] and by S.
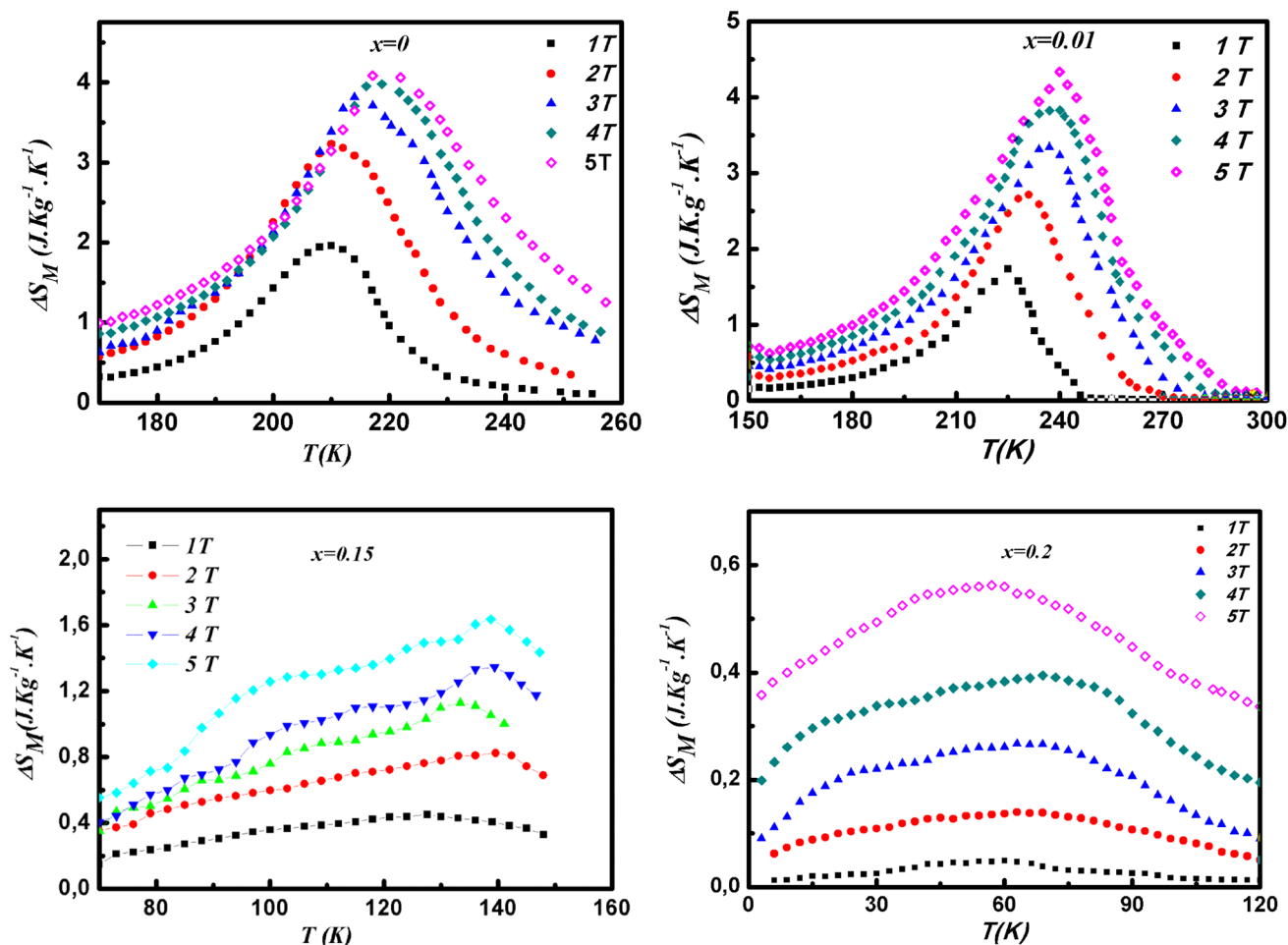
Fig. 7 Magnetic entropy change versus temperature for $La_{0.8}Ca_{0.2}Mn_{1-x}Fe_xO_3$ samples at several magnetic applied field changes: **a** $x = 0$, **b** $x = 0.01$, **c** $x = 0.15$, and **d** $x = 0.2$

Ghodhbane et al. for $Pr_{0.8}Ba_{0.2}MnO_3$ compounds under applied magnetic fields of 3 and 1 T, respectively. These values are lower than that of pure Gd [2.8 J/(kg K)] in a magnetic field change of 1 T [2]) and Gd_5 $(Si_xGe_{1-x})_4$ system [9] which have been considered as good magnetic refrigerants. For $LCMFe_{0.15}$ and $LCMFe_{0.2}$, the maximum value of magnetic entropy change, $\left|\Delta S_M^{max}\right|$, is 1.6 and 0.54 K/(kg K) under a magnetic field of 5 T, respectively. Similar results have been reported for $La_{0.7}Ca_{0.15}Sr_{0.15}$-$Mn_{0.9}Fe_{0.1}O_3$ [18] and $La_{0.63}Ca_{0.33}Mn_{0.8}Fe_{0.2}O_3$ [30].

The temperature dependence of the ΔS_M upon the magnetic applied field changes of 5 T is shown in Fig. 8. These curves reveal that the $La_{0.8}Ca_{0.2}Mn_{1-x}Fe_xO_3$ ($x = 0$, 0.01) samples present large magnetic entropy change and that ΔS_M decreases when increasing the Fe content (x). This behavior is understood as the reduction of the double-exchange mechanism between Mn^{3+} and Mn^{4+} ions for $La_{0.8}Ca_{0.2}Mn_{1-x}Fe_xO_3$ samples when x increases.

Relative cooling power (RCP)

Another useful parameter which examines the efficiency of a magnetocaloric material is the RCP or the refrigerant capacity. It expresses the heat transfer between the hot and the cold reservoirs during an ideal refrigeration cycle. This is defined as the product of peak value of change in the magnetic entropy and the full width at half maximum (FWHM) of ΔS_M versus T curve (Fig. 8, inset) [31].

$$RCP = -\Delta S_M^{max} \times \delta T_{FWHM} \qquad (3)$$

We have represented in Fig. 9 the variation of the RCP factor as a function of the applied magnetic field. The RCP values exhibit a linear rise with increasing field for LCMO and $LCMO_{0.01}$ samples. Under the influence of an applied field of 5 T, the RCP values are found to be 146 and 116 J/kg for the samples $x = 0$ and 0.01, respectively. Similar RCP values at 5 T (RCP = 140 J/kg) have been

Table 3 Maximum entropy change $\left|\Delta S_M^{max}\right|$ and relative cooling power (RCP) for $La_{0.8}Ca_{0.2}Mn_{1-x}Fe_xO_3$ ($x = 0$, 0.01, 0.15, 0.2) samples, occurring at the Curie temperature (T_C) under magnetic field variations, and compared to several materials considered for magnetic refrigeration

Composition	T_C (K)	ΔS_M (J/K kg)	μ_0H (T)	RCP (J/kg)	References
Gd	293	9.5	5	410	[2]
$La_{0.8}Ca_{0.2}MnO_3$	223	4.42	5	165	Our work
$La_{0.8}Ca_{0.2}Mn_{0.99}Fe_{0.01}O_3$	205	4.32	5	116	Our work
$La_{0.8}Ca_{0.2}Mn_{0.85}Fe_{0.15}O_3$	114	1.6	5	–	Our work
$La_{0.8}Ca_{0.2}Mn_{0.8}Fe_{0.2}O_3$	70	0.52	5	–	Our work
$La_{0.8}Ca_{0.2}MnO_3$ (annealed at 800 °C)	241	8.1	5		[22]
$La_{0.8}Ca_{0.2}MnO_3$ (polycrystalline, annealed at 1200 °C)	183	2.23	2	112.36	[23]
$La_{0.8}Ca_{0.2}MnO_3$ (single crystal)	176	3.67	1.5	99.09	[24]
$La_{0.8}Ca_{0.2}MnO_3$					[25]
$D = 17$ nm		0.6	4.5	140	
$D = 28$ nm		4.2	4.5	350	
$D = 43$ nm		8.63	4.5	225	
$Pr_{0.8}Ba_{0.2}MnO_3$	295	4.15	5	230	[26]
$La_{0.8}Cd_{0.2}MnO_3$	155	1.01	1.35	32	[27]
$Pr_{0.8}Pb_{0.2}MnO_3$	175	2.64	1.35	55	[28]
$La_{0.8}Ca_{0.2}Mn_{0.95}Fe_{0.05}O_3$	233	3	5	238	
$La_{0.67}Ca_{0.33}Mn_{0.85}Fe_{0.15}O_3$	147	3.21	5	–	[29]
$La_{0.7}Ca_{0.15}Sr_{0.15}Mn_{0.9}Fe_{0.1}O_3$	225	1.7	5	118	[30]
$La_{0.63}Ca_{33}Mn_{0.8}Fe_{0.2}O_3$	92	0.3	5	–	[31]

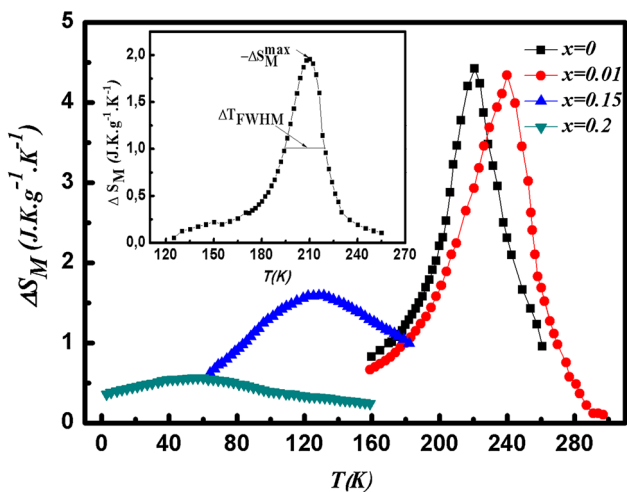**Fig. 8** Temperature dependence of the magnetic entropy change under an applied magnetic field of 5 T for $La_{0.8}Ca_{0.2}Mn_{1-x}Fe_xO_3$ compounds

Fig. 9 Variation of the relative cooling power as a function of the applied magnetic field for $La_{0.8}Ca_{0.2}Mn_{1-x}Fe_xO_3$ ($x = 0$ and $x = 0.01$) compound

reported for $La_{0.8}Ca_{0.2}MnO_3$ [26] and $La_{0.7}Ca_{0.15}Sr_{0.15}Mn_{0.9}Fe_{0.1}O_3$ samples [24]. Another interesting feature in the MCE plot is its asymmetric shape, especially under high field. Similar behavior is observed in Fe-substituted lanthanum calcium manganite [30]. For comparison, the maximum magnetic entropy change, the Curie temperature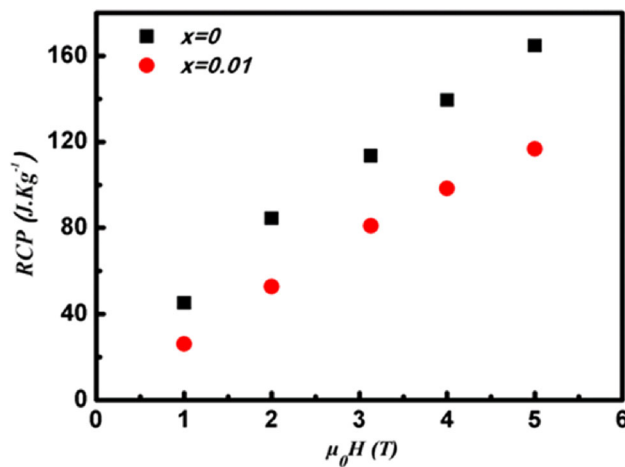, and the relative magnetic cooling efficiency of several manganese perovskites considered useful for room-temperature magnetic refrigerators are summarized in Table 3. Thus, due to the high ΔS_M and RCP values, our compounds with $x = 0$ and 0.01 could be considered as active magnetic refrigerants for near-room-temperature magnetic refrigeration.

Conclusion

We have studied the structural, magnetic, and magnetocaloric properties of the Fe-doped manganite perovskite $La_{0.8}Ca_{0.2}Mn_{1-x}Fe_xO_3$ compounds with $0 \leq x \leq 0.2$. The results show that the samples crystallize in the orthorhombic structure with Pnma space group. The magnetic properties reveal that all samples exhibit a paramagnetic–ferromagnetic transition when temperature decreases. From magnetocaloric study, the LCMO and $LCMF_{0.01}O$ samples have a large magnetic entropy change. The maximum values of the magnetic entropy changes decrease with the increase of Fe concentration. In addition, due to the high ΔS_M and RCP values, Fe-doped manganite perovskite samples can be considered a potential refrigerant for use in near-room-temperature magnetic refrigeration.

References

1. Warburg, E.: Magnetische untersuchung. Ann. Phys. **13**, 141–164 (1881)
2. Gschneidner, K.A., Pecharsky, V.K., Tsokol, A.O.: Recent developments in magnetocaloric materials. Rep. Prog. Phys. **68**, 1479–1539 (2005)
3. Bruck, E.: Developments in magnetocaloric refrigeration. J. Phys. D Appl. Phys. **38**, R381–R391 (2005)
4. Vitalij, K., Pecharsky, V.K., Gschneidner Jr, K.A.: Magnetocaloric effect and magnetic refrigeration. J. Magn. Magn. Mater. **200**, 4456 (1999)
5. Phan, M.H., Yu, S.C.: Review of the magnetocaloric effect in manganite materials. J. Magn. Magn. Mater. **308**, 325–340 (2007)
6. Tishin, A.M., Spichkin, I.: The Magnetocaloric Effect and Its Applications. Institute of Physics Publishing, Bristol (2003)
7. Gschneidner Jr, K.A., Pecharsky, V.K.: Advanced magnetocaloric materials: what does the future hold? Int. J. Refrig **29**, 1239–1249 (2006)
8. Atalay, S., Gencer, H., Kolat, V.S.: Magnetic entropy change in $Fe_{74-x}Cr_xCu_1Nb_3Si_{13}B_9$ (x= 14 and 17) amorphous alloys. J. Non-Cryst. Solids **351**(30), 2373–2377 (2005)
9. Pecharsky, V.K., Gschneidner Jr, K.A.: Giant magnetocaloric effect in $Gd_5(Si_2Ge_2)$. Appl. Phys. Lett. **70**, 3299 (1997)
10. Fujieda, S., Fujita, A., Fukamichi, K.: Large magnetocaloric effect in $La(Fe_xSi_{1-x})_{13}$ itinerant-electron metamagnetic compounds. Appl. Phys. Lett. **81**, 1276 (2002)
11. Tegus, Q., Bruck, E., Buschow, K.H.: Boer, F. R.: Transition-metal-based magnetic refrigerants for room-temperature applications. Nature **415**, 150 (2002)
12. Wang, F.W., Zhang, X.X., Hu, F.X.: Large magnetic entropy change in $TbAl_2$ and $(Tb_{0.4}Gd_{0.6})Al_2$. Appl. Phys. Lett. **77**, 1360 (2000)
13. Morelli, D.T., Mance, A.M., Mantese, J.V., Micheli, A.L.: Magnetocaloric properties of doped lanthanum manganite films. J. Appl. Phys. **79**, 373–375 (1996)
14. Guo, Z.B., Du, Y.W., Zhu, J.S., Huang, H., Ding, W.P., Feng, D.: Large magnetic entropy change in perovskite-type manganese oxides. Phys. Rev. Lett. **78**, 1142 (1997)
15. Guo, Z.B., Zhang, J.R., Huang, H., Ding, W.P., Du, Y.W.: Lattice effect in Pr doped La Sr Mn O perovskite. Solid State Commun. **100**, 769–771 (1996)
16. Hueso, L.E., Sande, P., Miguens, D.R., Rivas, J., Rivadulla, F., Lopez-Quintela, M.A.: Tuning of the magneto-caloric effect in $La_{0.67}Ca_{0.33}MnO_{3-\delta}$ nanoparticles synthesized by sol-gel techniques. J. Appl. Phys. **91**, 9943 (2002)
17. Rodrigez-Carjaval, J.: XVth congess of the international union of crystallography. In: Proceedings of the satellite meeting on powder diffraction, vol. 127.Toulouse (1990)
18. Othmani, S., Blel, R., Bejar, M., Sajieddine, M., Dhahri, E., Hlil, E.K.: New complex magnetic materials for an application in Ericsson refrigerator. J. Solid State Commun. **149**, 969–972 (2009)
19. Issaoui, F., Tlili, M.T., Bejar, M., Dhahri, E., Hlil, E.K.: Structural and magnetic studies of $Ca_{2-x}Sm_xMnO$ compounds (x = 0–0.4). J. Supercond. Novel. Mag. **25**(4), 1169–1175 (2012)
20. Banerjee, S.K.: On a generalised approach to first and second order magnetic transitions. Phys. Lett. **12**, 16–17 (1964)
21. Foldeaki, M., Chahine, R., Gopal, B.R., Bose, T.K.: Investigation of the magnetic properties of the $Gd_{1-x}Er_x$ alloy system in the x < 0.62 composition range. J. Magn. Magn. Mater. **150**(3), 421–429 (1995)
22. Nisha, P.: Pilla, i S.S., Varma, M.R., Surech, K.G.: Critical behavior and magnetocaloric effect in $La_{0.67}Ca_{0.33}Mn_{1-x}Cr_xO_3$ (x = 0.1, 0.25). Solid State Sci. **14**, 40–47 (2012)
23. Khlifi, M., Bejar, M., Sadek, O.E.L., Dhahri, E., Ahmed, M.A., Hlil, E.K.: Structural, magnetic and magnetocaloric properties of the lanthanum deficient in $La_{0.8}Ca_{0.2-x-x}MnO_3$ (x = 0–0.20) manganites oxides. J. Alloy. Compd. **509**, 7410–7415 (2011)
24. Phan, M.H., Phan, V.T., Yu, S.C., Rhee, J.R., Hur, N.H.: Excellent magnetocaloric properties of $La_{0.7}Ca_{0.3-x}Sr_xMnO_3$ (0.05-x-0.25) single crystals. Appl. Phys. Lett. **86**, 072504 (2005)
25. Xi, S., Lu, W., Sun, Y.: Magnetic properties and magnetocaloric effect of $La0·8Ca0·2MnO_3$ nanoparticles tuned by particle size. J. Appl. Phys. (2012). doi:10.1063/1.3699037
26. Ghodhbane, S., Dhahri, A., Dhahri, N., Hlil, E.K., Dhahri, J.: Structural, magnetic and magnetocaloric properties of $La_{0.8}Ba_{0.2}Mn_{1-x}Fe_xO_3$ compounds with $0 \leqslant x \leqslant 0.1$. J. Alloy. Compd. **550**, 358–364 (2013)
27. Gschneidner, K.A., Pecharsky, V.K.: Magnetocaloric materials. Annu. Rev. Mater. Sci. **30**, 387 (2000)
28. Phan, M.H., Peng, H.X., Yu, S.C., Hanh, D.T., Tho, N.D., Chau, N.: Structure, magnetic, magnetocaloric and magnetoresistance properties of $Pr_{1-x}PbxMnO_3$ perovskites. J. Appl. Phys. **Q108**, 9908 (2006)
29. Nisha, P., Pillai, S.S., Vacma, M.R., Surech, K.G.: Influence of cobalt on the structural, magnetic and magnetocaloric properties of $La_{0.67}Ca_{0.33}MnO_3$. J. Magn. Magn. Mater. **327**, 189–195 (2013)
30. Nisha, P., Pillai, S.S., Darbandi, A., Varma, M.R., Suresh, K.G., Hahn, H.: Critical behavior and magnetocaloric effect in nano crystalline $La_{0.67}Ca_{0.33}Mn_{1-x}FexO_3$ (x = 0.05, 0.2) synthesized nebulized spray pyrolysis. Mater. Chem. Phys. **136**(1), 66–74 (2012)
31. Kamilov, I.K., Gamzatov, A.G., Aliev, A.M., Batdalov, A.B., Aliverdiev, A.A., Abdulvagidov, ShB, Melnikov, O.V., Gorbenko, OYu., Kaul, A.R.: Magnetocaloric effect in $La_{1-x}Ag_y$-MnO_3 ($y \leq x$): direct and indirect measurements. J. Phys. D **40**, 4413 (2007)